Hindawi
Geofluids
Volume 2023, Article ID 3658141, 16 pages
https://doi.org/10.1155/2023/3658141

Research Article

Evolution Mechanism and Control of Floor Heave in the Deep Roadway with Retained Bottom Coal

Peng Li[1,2] **Yonglu Suo**[1] **Peilin Gong**[3] **Xingping Lai**[1] **Kang Yi**[4,5] **Chao Su**[3,5] **and Chang Liu**[5]

[1]*Energy School Xi'an University of Science and Technology, Xi'an 710054, China*
[2]*Department of Mining Engineering, Shanxi Institute of Energy, Jinzhong 030600, China*
[3]*College of Mining Technology, Taiyuan University of Technology, Taiyuan 030024, China*
[4]*School of Energy & Mining Engineering, China University of Mining and Technology (Beijing), Beijing 100083, China*
[5]*Mining and Designing Branch, China Coal Research Institute, Beijing 100013, China*

Correspondence should be addressed to Yonglu Suo; shiya@xust.edu.cn and Peilin Gong; plgong@126.com

Received 21 May 2021; Revised 31 July 2021; Accepted 23 September 2021; Published 22 March 2023

Academic Editor: Yong-Zheng Wu

Roadways with retained bottom coal are common in thick coal seam mining, and floor heaving is a prominent problem. In this study, based on the interaction between the floor and two sides of the roadway-surrounding rock, a Winkler elastic foundation beam model is established to analyze the floor heave problem. A 3DEC model was used to analyze the failure range, failure mode, and migration law of the floor-surrounding rock with different bottom coal thicknesses and coal body strengths. The results show that (1) an increase in the thickness of the bottom coal results in a decrease in the stiffness of the roadway side coal body (the foundation of the supporting rock layer) and an increase in the bending deformation range, the amount of floor rock beam deformation, and the extrusion force. This leads to an expansion in the range of the sides of the coal body that are squeezed by the floor rock layer, resulting in additional failure and deformation of the coal body sides. Therefore, the damage to the floor rock layer is extended and increased. (2) The expansion of the floor pressure-bearing arch and surrounding rock in the arch are the causes of floor heave in the deep coal roadway with retained bottom coal. (3) Because of an increase in the thickness of the bottom coal and a decrease in the coal body strength, the floor pressure-bearing arch expands to the deeper part; thus, the range of surrounding rock in the arch with deformation and failure increases, resulting in an increase in floor heave. The field practice indicates that the support strategy of the "high prestressed strong rock bolt (cable) supporting two sides and bottom corners in time" can effectively control the floor heave of a roadway with retained bottom coal.

1. Introduction

With the development of deeper coal resources in recent years [1–3], the buried depth of roadways has been increasing. Deep roadways account for 30% of the roadways excavated every year in China, of which 70% need to be repaired due to large deformations, greatly increasing production costs [4]. Compared to the roof and two sides, the roadway floor usually exhibits greater deformation because it often lacks support [5, 6]. Roadways with retained bottom coal are often used in thick coal seam mining, and their weak floor can result in very serious floor heave [7].

There are two main factors that cause floor heaving in coal mine roadways. The first factor, in situ stress, is the local stress resulting from roadway excavation. Radial unloading and shear loading are the main causes of deformation and failure in the surrounding rock [8–10]. For the floor, an increase in horizontal in situ stress—as the initial value of tangential stress—aggravates the deformation and failure of the rock mass [11, 12]. Roadway floor heave is also induced by the mining stress from coal mining activities [13, 14]. The second factor includes the characteristics of the floor rock mass; a high elastic modulus and strength of the floor rock mass both reduce the amount of floor heave. Whereas, an

increase in floor rock mass discontinuity leads to an increase in floor heave [7, 15]. The floor rock mass also deteriorates as water from the floor and roadway passes through the fault fracture zone [16, 17], further increasing floor heave [18].

Control of roadway floor heave should start with the two factors listed above [19, 20]. The first is stress control. Optimizing the mining layout and implementing slotting in the floor can reduce the stress level of the floor rock mass, thus controlling floor heave [21]. Alternatively, floor heave can also be reduced by strengthening the floor rock mass. The strength of the floor rock mass can be improved by installing floor bolts [22–24], constructing a concrete inverted arch [25, 26], or modifying floor grouting [27, 28].

Most of the papers referenced above focus only on the floor itself. However, the floor and the surrounding rock should be understood as a single unit. Therefore, the deformation and failure of the roof and roadway sides also affects the floor [29]. Additionally, it is difficult to strengthen the floor by drilling holes to install bolts or by modifying floor grouting, and constructing a concrete inverted arch is expensive and time consuming. Therefore, the mechanism of floor heave should be further studied to develop more efficient support methods.

The accumulated floor heave was more than 2 m before mining in No. 020202 roadway of the Qingyun coal mine, Jiexiu, Shanxi Province. The roadway floor heave was controlled by removing the bottom coal and adding bolts and cables to the bottom corners of the roadway.

This study uses theoretical analysis, physical similarity simulation, and field observation to comprehensively evaluate the evolution mechanism and control of floor heave in a deep roadway with retained bottom coal. This study establishes a mechanical model to evaluate the influence of bottom coal on the deformation and failure of floor rock using the No. 020202 tailgate of the Qingyun mine as the research subject. The evolution mechanism of floor heave caused by the floor expansion of a roadway with retained bottom coal is studied using numerical simulations. A new support method and parameters are proposed based on the deformation and migration of floor rock strata. Field practice confirms that roadway floor heave is controlled using the new support method.

2. Project Background

The 020202 working face of the Qingyun coal mine was mining the No. 2 coal seam. There were no mining activities or goafs around the working face, as shown in Figure 1. The No. 020202 tailgate of the Qingyun mine had a buried depth of 792–810 m, classifying it as a deep roadway [30]. The roadway was excavated along the roof of the No. 2 coal seam with a width of 4.5 m and a height of 3.8 m. A rock bolting system was adopted, including rock bolts with a length of 3000 mm, a diameter of 20 mm, a preload of about 10-20 kN, and a row spacing of 800 mm (11 rock bolts per row), as well as cables with a diameter of 17.8 mm, a length of 6200 mm, a preload of about 50-60 kN, and a row spacing of 1600 mm (8 cables per row). The physical and mechanical properties of the rock surrounding the roadway are listed in Table 1.

Before mining, the deformation of the No. 020202 tailgate was serious, with large displacements on the two sides of the roadway and serious floor heave. However, the roof was complete, and its displacement was small. The cumulative floor heave was more than 2 m, as shown in Figure 2, seriously restricting safe production.

The thickness of the floor coal of roadway No. 020202 was 1.3 m. The floor heave caused by floor coal crushing was only 0.26 m with a crushing expansion coefficient of 1.2, far less than the cumulative floor heave of the roadway. Therefore, the deformation and failure of the floor rock of the roadway was inevitable. The floor heave was not only related to the deformation of the floor itself but was also related to the deformation of the two sides. The low strength of the surrounding rock on the two sides also increased floor heave.

3. Deformation and Failure Mechanism of the Floor in the Deep Roadway with Retained Bottom Coal

3.1. Reverse Foundation Model of Roadway Floor. When the roadway was excavated, the floor rock beam bent under the action of ground stress from the roadway. Therefore, an elastic foundation beam model was used to analyze the deformation of the roadway floor, as shown in Figure 3. The coal body on the two sides of the roadway was the elastic foundation (the roof was hard and anchored, so it can be assumed that the roof deformation was small). The rock beam and foundation used in the elastic foundation model were elastic bodies. To simplify the conditions for semiquantitative analysis, the elastic modulus of the coal body in the plastic zone of the roadway side was approximated.

Assuming that the rock and coal in the floor conform to the Winkler foundation hypothesis [31], the vertical force p in the coal body satisfies the following conditions:

$$p = -ky, \tag{1}$$

where p is the vertical force in the coal seam, k is the foundation coefficient of the coal seam, and y is the deformation of the coal seam induced by p.

According to Timoshenko's solution, the differential equations that describe the floor rock beam bending deformation are [32] as follows:

$$\mathrm{EI}y'''' + Ny'' = q_z \text{ for } -(l + b_1) \le x < -b_1, \tag{2}$$

$$\mathrm{EI}y'''' + Ny'' = q_1(x) - k_1 y \text{ for}(-b_1 \le x < 0), \tag{3}$$

$$\mathrm{EI}y'''' + Ny'' = q_2(x) - k_2 y \text{ for}(0 \le x < b_2), \tag{4}$$

where EI is the stiffness of the floor rock stratum, k_2 is the foundation coefficient of the complete coal body, k_1 is the coefficient of the parallel foundation between the coal body with support and the bottom coal without support, q_z is the load of the exposed floor rock beam, q_0 is the load of

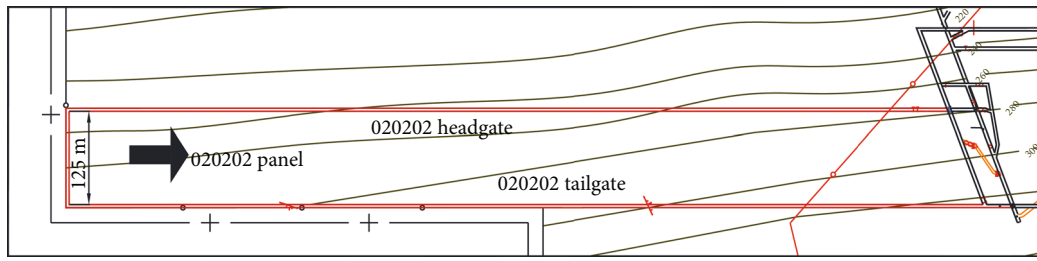

Figure 1: Layout of the No. 020202 panel of Qingyun coal mine.

Table 1: Physical and mechanical properties of the surrounding rock.

Stratum lithology	The average thickness (m)	Bulk modulus (GPa)	Shear modulus (GPa)	Tensile strength (MPa)	Cohesion (MPa)	Frictional angle (°)
Compound roof	18.5	13.6	3.7	3.5	12.1	27
Siltstone	3.7	10.3	3.1	3.7	9.2	26
Mudstone	2.3	7.9	2.1	1.1	3.2	23
Siltstone	2.9	16.2	5.3	3.3	7.2	26
Medium sandstone	2.3	13.2	3.7	5.2	13.1	29
No. 2 coal	5.1	3.7	1.3	0.6	2.3	27
Sandy mudstone	5.7	8.8	3.6	2.5	3.2	21
No. 4 coal	0.9	3.7	1.3	0.6	2.3	27
Siltstone	1.9	12.7	3.1	3.2	6.7	26
Fine-grained sandstone	3.3	12.9	2.6	2.1	3.3	23
Compound floor	18.0	9.7	2.6	2.7	3.1	27

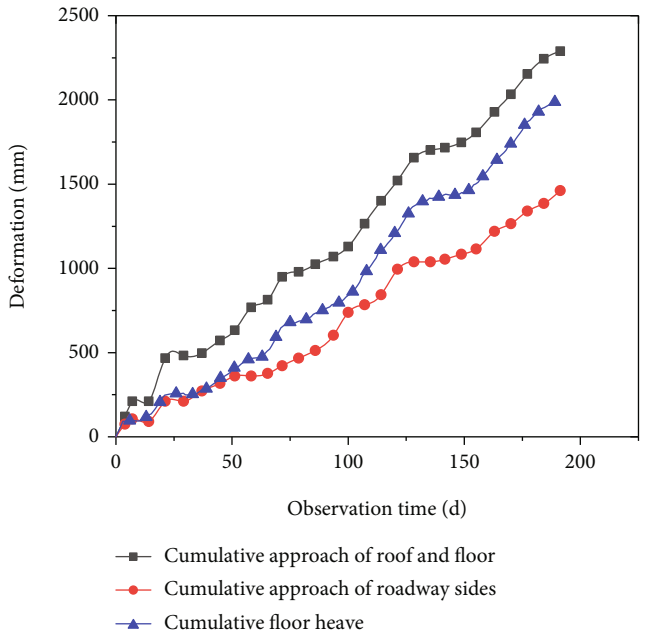

Figure 2: Deformation of the No. 020202 tailgate of Qingyun mine with the original support.

the exposed floor rock beam, q_v is the load of the exposed floor rock beam, $q_{1(x)}$ is the function formula of the stress in the floor rock beam, $q_{2(x)}$ is the function formula of the stress in the floor rock beam, y is the deformation of the coal seam, l is one-half of the width of the roadway, b_1 is the plastic zone width of the roadway, and b_2 is the stress increased zone width of the roadway. When the entire rigid displacement load is not considered, the load can be calculated as follows:

$$q_2(x) = \frac{b_2 - x}{b_2}(q_0 - q_v), \tag{5}$$

$$q_1(x) = \frac{q_0 - q_z - q_v}{b_1}x + q_0 - q_v. \tag{6}$$

The expression $y(x)$ can be obtained using the differential equation.

When the elastic foundation beam model is adopted, it must be assumed that the plastic zones on both sides of the roadway $-b_1 \le x < 0$ obey the law of elastic deformation. The foundation coefficient is k_2 in the elastic zone and k_1 in the plastic zone, as follows:

$$k_1 = \frac{k_{11}k_{12}}{k_{11} + k_{12}}, \tag{7}$$

where k_{11} is the foundation coefficient after the installation of the bolt support, and k_{12} is the foundation coefficient of the bottom coal in the plastic zones of the two sides of the roadway without bolt support. It should be noted that the

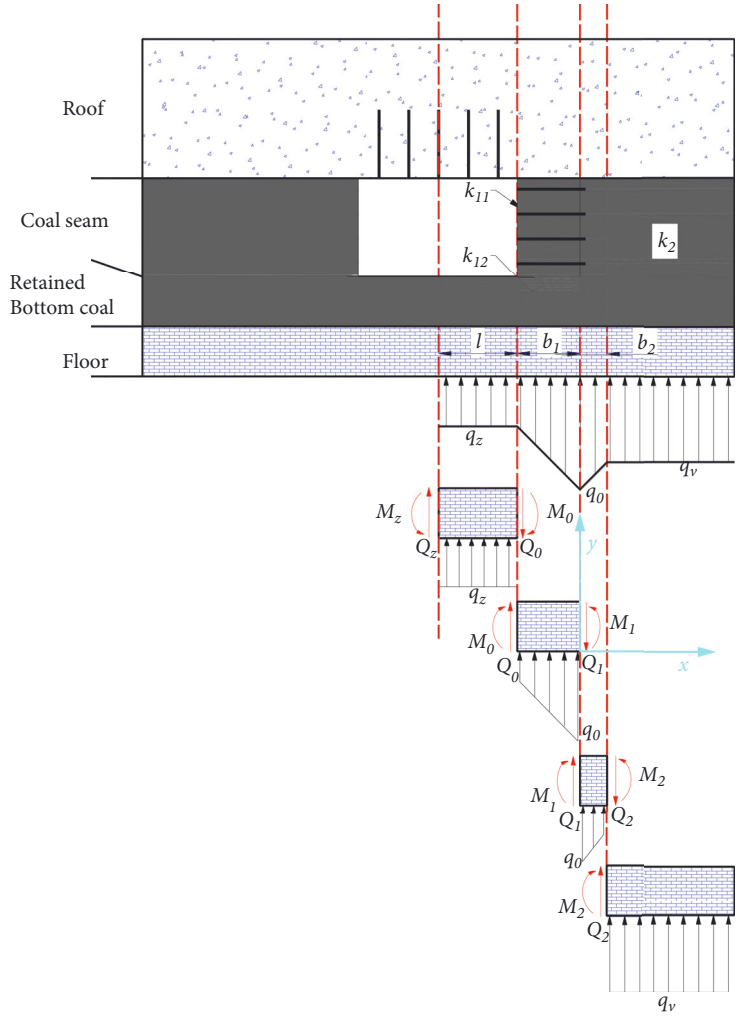

Figure 3: Reverse foundation model of the roadway floor.

value of the foundation coefficient k_{12} of the coal wall in the plastic zone is expressed by an average empirical value smaller than the foundation coefficient k_2 of the complete coal body.

Generally,

$$k = \frac{E}{h}, \tag{8}$$

where h is the thickness of the foundation, E is the elastic modulus of the foundation, and the equivalent elastic modulus of the coal body supported by the bolt can be calculated according to the following formula [33–35]:

$$E_{11} = E_{12} + \frac{\pi {d_b}^2 E_b}{4 S_\theta S_r}, \tag{9}$$

where d_b is the diameter of the bolt, E_b is the stiffness of the bolt, and S_θ and S_r are the radial and axial bolt spacings, respectively.

In equation (9), the equivalent elastic modulus is composed of the elastic modulus of coal in the plastic zone and the stiffness of the bolt support. If the bolt support is implemented before plastic deformation of the surrounding rock, then the plastic deformation of the two sides of the coal body can be effectively limited. As a result, the elastic modulus of the coal body increases, better controlling the deformation of the surrounding rock.

When $x \geq 0$, there is no support and no plastic failure in the coal. The displacement of the semi-infinite foundation beam under the unknown moment and shear force, M_1 and Q_1, at $x = 0$ is as follows:

$$y_b(x) = \frac{2\beta_2}{k_2}[Q_1\theta(x) + \beta_2 M_1 \psi(x)], \tag{10}$$

where $\psi(x)$, $\theta(x)$, $\varphi(x)$, and $\xi(x)$ are function formulas and β_2 is a constant, as described here:

$$\begin{aligned} \varphi(x) &= e^{-\beta_2 x}[\cos \beta_2 x + \sin \beta_2 x], \\ \psi(x) &= e^{-\beta_2 x}[\cos \beta_2 x - \sin \beta_2 x], \\ \theta(x) &= e^{-\beta_2 x} \cos \beta_2 x, \\ \xi(x) &= e^{-\beta_2 x} \sin \beta_2 x. \end{aligned} \tag{11}$$

$$\beta_2 = \sqrt[4]{\frac{k_2 b}{4\mathrm{EI}}}. \tag{12}$$

As shown in Figure 3, the displacement of the semi-infinite beam under a distributed load should also be considered.

When $x \geq b_2$, it is

$$y_2(x) = \frac{2\beta_2}{k_2}[Q_1\theta(x) + \beta_2 M_1\psi(x)] + \frac{q_0 - q_v}{4k\beta_2 b_2}[\psi(x\text{-}b_2) - 2\xi(b_2)\theta(x) - \varphi(b_2)\psi(x)]. \tag{13}$$

When $0 \leq x < b_2$, it is

$$y_1(x) = \frac{2\beta_2}{k_2}[Q_1\theta(x) + \beta_2 M_1\psi(x)] + \frac{q_0 - q_v}{4k\beta_2 b_2} \cdot [4\beta_2(b_2 - x) + \psi(b_2 - x) - 2\xi(b_2)\theta(x) - \varphi(b_2)\psi(x)]. \tag{14}$$

When $-b1 \leq x < 0$, the coal body is strengthened by bolt support, the bottom coal is plastic damaged, the foundation coefficient of the coal body changes, and the displacement of the floor strata can be calculated as a finite-length foundation beam as follows:

$$y_0(x) = y_a F_1(x) - \frac{\theta_a}{\beta_1} F_2(x) + \frac{M_a}{{\beta_1}^2\mathrm{EI}} F_3(x) + \frac{Q_a}{{\beta_1}^3\mathrm{EI}} F_4(x) - \frac{M_0}{{\beta_1}^2\mathrm{EI}} F_3(x + \mathrm{b}_1) - \frac{Q_0}{{\beta_1}^3\mathrm{EI}} F_4(x + \mathrm{b}_1) - \frac{1}{{\beta_1}^3\mathrm{EI}} \int_0^{-x} \left[\frac{q_0 - q_z - q_v}{b_1}\mathrm{t} + (q_z - q_v)\right] F_4(x + \mathrm{t})dt, \tag{15}$$

where y_a, θ_a, M_a, and Q_a are the transition parameters for displacement, rotation angle, bending moment, and shear force, respectively, at $x = 0$ when there is no other external force, and

$$\begin{aligned} F_1(x) &= ch(\beta_1 x)\cos(\beta_1 x), \\ F_2(x) &= \frac{1}{2}[ch(\beta_1 x)\sin(\beta_1 x) + sh(\beta_1 x)\cos(\beta_1 x)], \\ F_3(x) &= \frac{1}{2}sh(\beta_1 x)\cos(\beta_1 x), \\ F_4(x) &= \frac{1}{4}[ch(\beta_1 x)\sin(\beta_1 x) - sh(\beta_1 x)\cos(\beta_1 x)]. \end{aligned} \tag{16}$$

When $-l - b1 \leq x < -b1$, the foundation coefficient is zero, and the bending moment of the rock deformation is

$$M(x) = M_z + \frac{1}{2}q_z(l + x)^2, \tag{17}$$

where q_z calculates the load of exposed floor rock beam.

By using $\mathrm{EI}y^{(2)} = M$ and the deformation compatibility conditions at $x = -l - b_1$ in the middle of the beam and $x = -b1$ and $x = 0$ at the ends of the beam, the deformation curve and bending moment equation of the floor can be calculated.

Based on the physical and mechanical parameters of the surrounding rock and in situ stress of the roadway, the deformation and bending moment of the floor rock without failure in the roadway were calculated when the bottom coal thicknesses were 0 m, 2 m, and 4 m, and where the vertical stress of the roadway is $q_v = \gamma H = 21.87$MPa. The stress concentration factors on the two sides of the roadway were both 1.5. As the roadway was excavated, the roof load was $q_z = 5$ MPa. The widths of the plastic zone and stress reduction zone were calculated to be 2 m and 4 m, respectively. The elastic moduli of the floor rock, coal body, and plastic zone of the coal body are 10 GPa, 3.7 GPa, and 1.1 GPa, respectively. The increase in the elastic modulus of the coal after the addition of supports was calculated using equation (9) and reference [36].

3.2. Influence of Different Bottom Coal Thickness on Crossfeed Action between Floor and Two Sides. By excavating the roadway to obtain different bottom coal thicknesses, the deformation and bending moment of the floor rock could be calculated. As the bottom coal thickness increases from 0 m to 4 m, the bending deformation and maximum bending moment of the floor rock increases significantly, as shown in Figure 4. Compared to the maximum deformation and maximum bending moment with a bottom coal thickness of 0 m, the maximum deformation of the floor rock bottom coal with thicknesses of 2 m and 4 m increases by 45% and 83%, respectively, and the maximum bending moment of the floor rock increases by 24% and 29%, respectively.

As shown in Figure 4(a), the zone $x > -2$ is the coal body zone on the roadway side. The deformation range of the roadway floor is below the roadway and 6–10 m from the roadway side. When the bottom coal thickness is 0 m, 2 m, and 4 m, the extended depth of the floor deformation range from the roadway side to the deep surrounding rock is 8.94 m, 9.86 m, and 10.57 m, respectively, and the deformation accounts for 89%, 90%, and 91% of the total deformation, respectively. Combined with Figure 5, it can be observed that, after the excavation of the roadway, the floor coal strength is at its lowest, and no support is applied. Because of the high stress of the deep surrounding rock, the floor coal fails first, and the floor rock is then unloaded. The floor rock bends under the action of in situ stress and bulges into the roadway. The deformation of the floor rock squeezes the bottom coal on both sides. If the support is not applied in time, the coal in the plastic zone of the two sides will further deteriorate, expand, and migrate into the roadway. This, in turn, weakens the bearing foundation of the floor rock, reduces the "span increasing" effect of the equivalent rock beam, causes the floor rock to further bend, aggravates the damage of the floor rock, and converts a larger range of rock into a plastic failure state.

As shown in Figure 4(b), the bending moment of the floor rock increases with an increase in the thickness of the

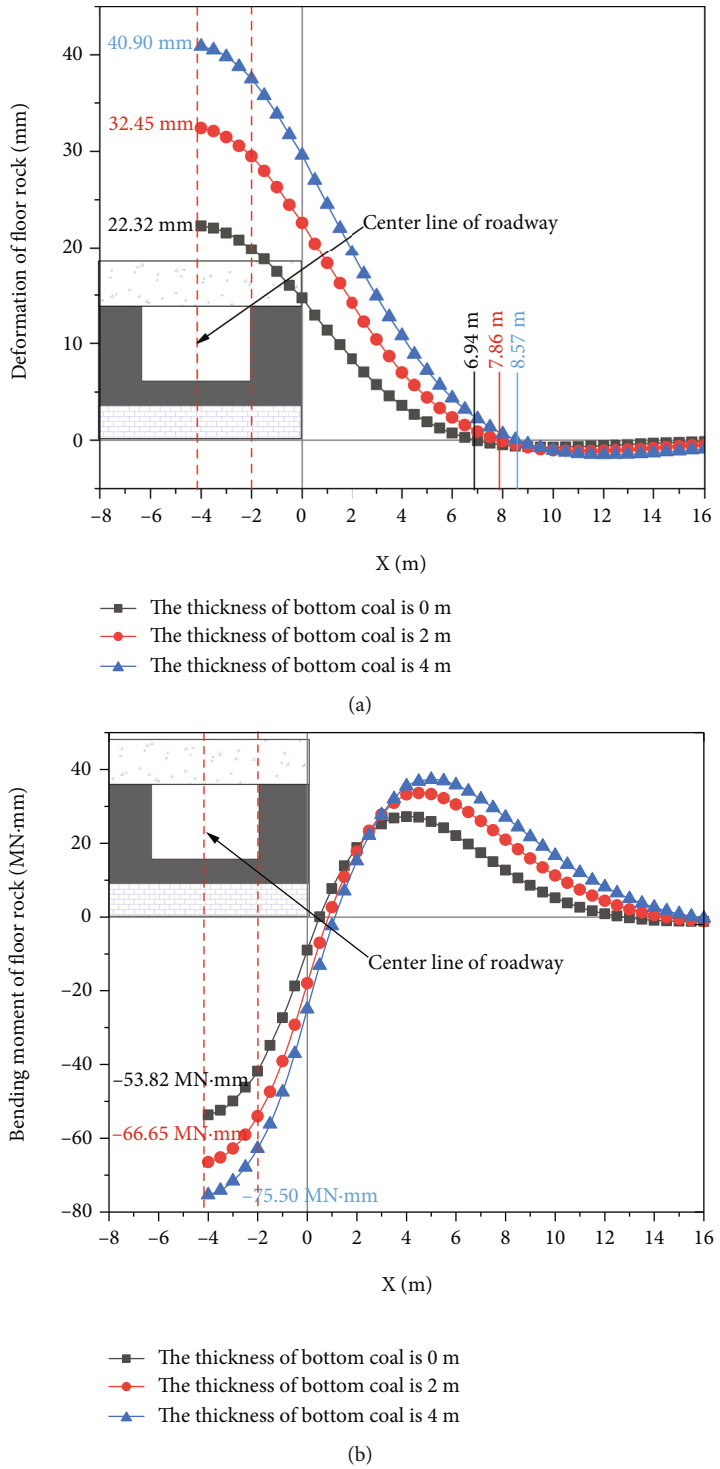

Figure 4: Deformation and bending moment of the floor rock under different thicknesses of the bottom coal. (a) Deformation of the floor rock. (b) Bending moment of the floor rock.

bottom coal, eventually causing the floor rock to break, first in the middle, and then at the end, forming a broken rock block.

As shown in Figure 4, an increase in the thickness of the bottom coal decreases the stiffness of the coal body (the foundation of the supporting rock layer), while the bending deformation range, deformation of the floor rock layer, and extrusion force all increase. This leads to an expansion in the range of the sides of the coal body that are squeezed by the floor rock layer, resulting in additional failure and deformation of the two sides of the coal body. Consequently, the damage to the floor rock layer is extended and increased. With an increase in the range of rock mass in the plastic failure state, roadway floor heave significantly increases.

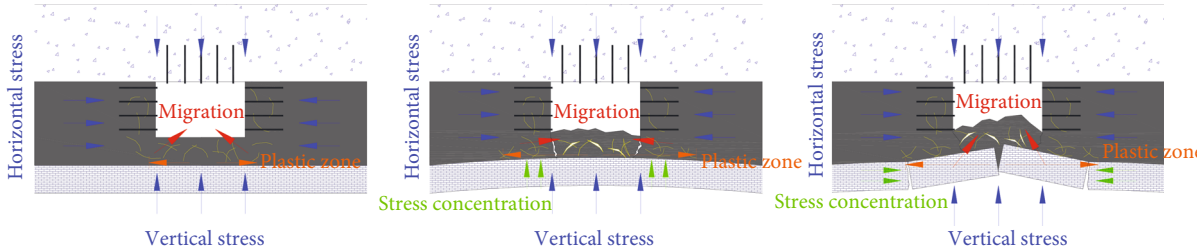

Figure 5: Migration evolution of floor-surrounding rock.

3.3. Influence of Different Support Strategies on Crossfeed Action between Floor and Two Sides. Figure 6 shows the deformation and bending moment of the roadway floor strata when the bottom coal thickness is 2 m while applying different support strategies. When close support is adopted, it is assumed that the plastic zone of the two sides is effectively controlled, and the elastic modulus of the coal in the plastic zone is the same as the elastic modulus of the coal body that is not damaged. The increase in the elastic modulus of the coal body with prestressed and non-pre-stressed supports is determined according to equation (9) and reference [36]. The foundation coefficients of the two sides of the coal body before and after the bottom corner support is installed are calculated according to equation (7) and equation (8).

Compared to the nontimely and non-pre-stressed support of the roadway side without supporting the bottom angle, the maximum deformation and bending moment of the floor rock with timely and prestressed support of the roadway side and the addition of a bottom angle support were reduced by 33% and 36%, respectively, while the maximum deformation and bending moment of the floor rock with timely and prestressed support of the roadway side but without the bottom angle support were both reduced by 13%. Therefore, supporting the bottom angle can effectively control the floor rock deformation of the roadway with retained bottom coal.

The maximum deformation and maximum bending moment of the floor rock with timely prestressed support of the roadway side and installed bottom angle support were reduced by 27% and 32%, respectively, compared to untimely prestressed support of the roadway side and with bottom angle supports installed. Conversely, when timely prestressed support of the roadway side is applied, but a supporting bottom angle is not used, the maximum deformation and bending moment of the floor rock are both reduced by 13% compared to untimely prestressed support of the roadway side without the bottom angle support installed. Therefore, timely support can effectively reduce the deformation and stress of the floor rock after roadway excavation.

The timely application of prestressed two-side support and bottom angle support after the excavation of a roadway with retained bottom coal can effectively improve the stiffness of the two sides of the roadway, reduce the damage range of the floor rock, and reduce the damage to the surrounding rock.

4. Evolution Mechanism of Floor Heave in the Deep Roadway with Retained Bottom Coal

Using the elastic foundation beam model, the induced effect of bottom coal on the deformation and failure of the floor rock and the two sides of the roadway are analyzed. Because the failure deformation of the floor rock is not equal to floor heave, it is necessary to study the mechanism of floor heave evolution caused by surrounding rock migration after the failure of the floor rock and floor sides.

4.1. Establishment of the Numerical Model. According to geological data and optical observation results in the borehole of the Qingyun mine, a plane model was established. The model size is $x = 64.5$ m in the direction of the roadway width and $z = 64$ m in the direction of the roadway height. To reduce the error, the model boundary was set 30 m from the roadway boundary. Because a continuous medium is conducive to applying more accurate boundary conditions, whereas a discrete medium is more suitable for simulating large deformations (because large deformations of deep roadway-surrounding rock are discontinuous and structural [37], many studies have adopted this method [38, 39]), the plane model was divided into two parts: the discrete medium is within 10 m of the roadway (greater than the range of significant deformation of the surrounding rock), and the rest is a continuous medium. To tailgate floor heave, the sandy mudstone floor with a thickness of 5.7 m was divided into 12 different colored layers (the physical and mechanical properties of the 12 layers are the same). The Mohr-Coulomb model was used to analyze and calculate the rock blocks and joints in the model. Considering gravitational acceleration $g = 9.81\ \mathrm{m/s^{-2}}$, the bottom of the model was fixed, the normal displacement of the side of the model was limited, and the stress boundary condition was used at the top of the model to replace the overburden weight. When the distribution law of rock joints is unknown, the rock block and joint surface in the 3DEC model were assigned a uniform strength and stiffness, representing the allowable cracking position in the model [40].

In this study, the influence of bottom coal on the movement of surrounding rock in the roadway was simulated to determine the influence of coal strength and bottom coal thickness. In the Mohr-Coulomb model, the strength of the coal seam and floor primarily depends on the cohesion and internal friction angle. However, in this instance, the amount of change in the internal friction angle was small.

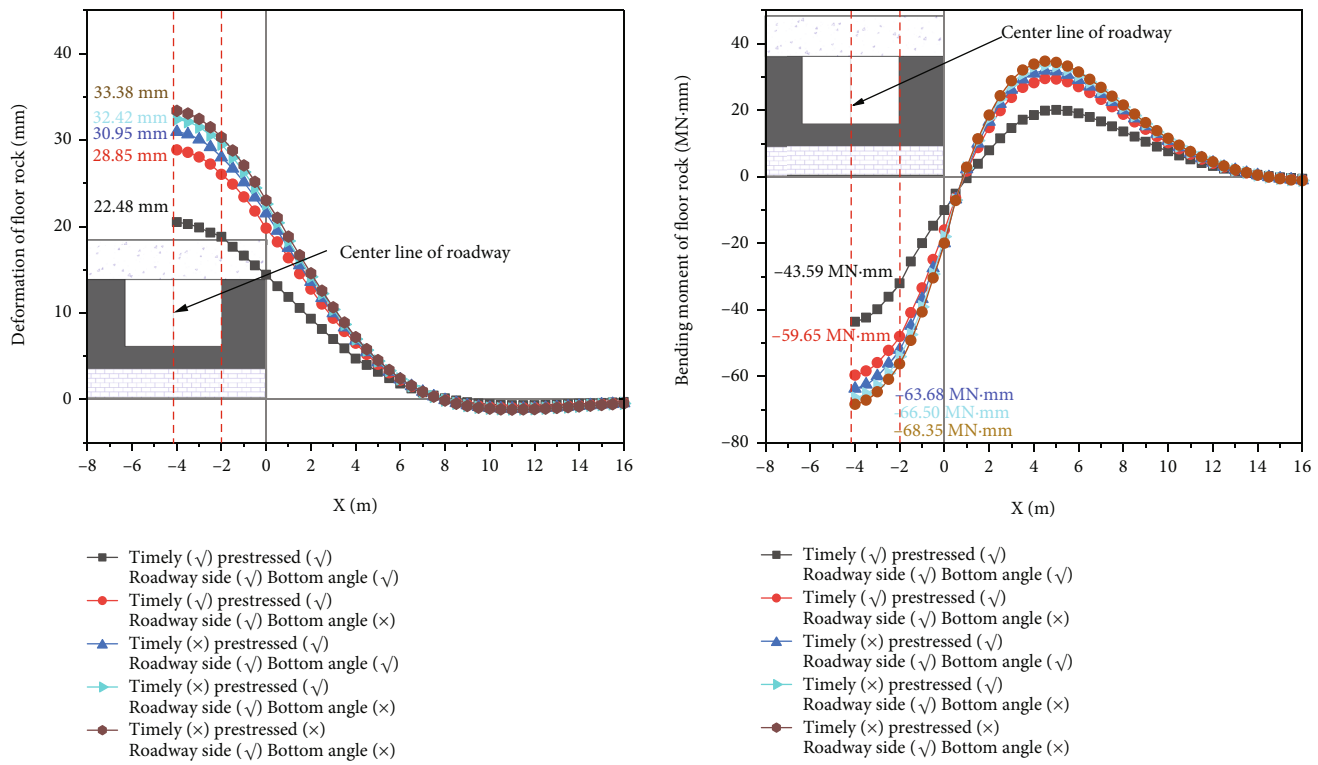

Figure 6: Deformation and bending moment of the floor rock under different support strategies.

Therefore, we simplified the model by assuming that the coal seam and floor strength were only influenced by cohesion. Based on the geological conditions of the No. 020202 tailgate of the Qingyun coal mine, three parameters were set for each factor in the range of common values: the thickness of the bottom coal was 0 m, 2 m, and 4 m; the cohesion of the coal body was 1 MPa, 3 MPa, and 5 MPa; and other mechanical parameters of the surrounding rock were set according to Table 1. Five simulation schemes were used in this study. Taking the bottom coal thickness of 0 m as an example, the numerical model is shown in Figure 7.

4.2. Expansion Law of the Bottom Arch in the Roadway with Retained Bottom Coal. Because the stress environment of the roadway floor is similar to that of the roadway roof, no difference was observed when comparing the deformation and failure of the floor-surrounding rock to that of the roof-surrounding rock. Therefore, it can be assumed that a bearing arch—similar to the one that formed when the roof-surrounding rock was destroyed—was also formed on the floor [41]. The floor rock mass did not collapse, but floor heave did occur. The numerical simulation results shown in Figure 8 better demonstrate this point. The evolution of the stress tensor with numerical steps in the surrounding rock of the retained bottom coal roadway is shown in Figure 9. When the roadway was excavated, the stress of the surrounding rock was redistributed, and stress deflection occurred at the shoulder angle and bottom angle of the roadway, forming the bearing arch. Stress was transferred to the arch foot through the bearing arch.

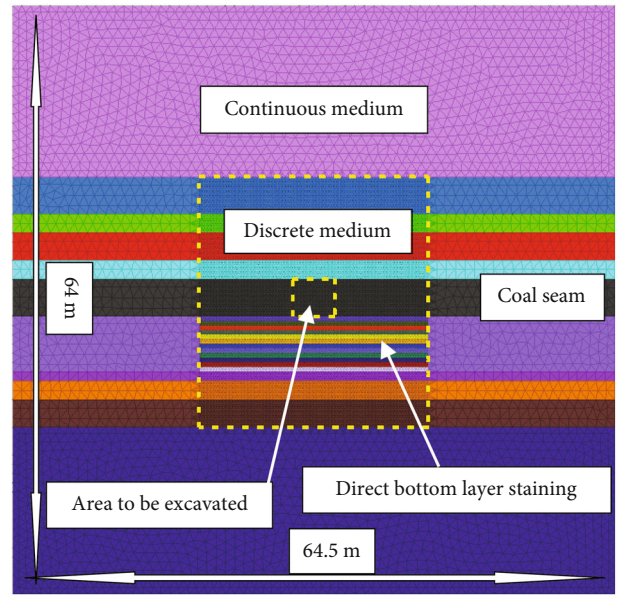

Figure 7: Numerical model.

The movement of the arch foot position in the horizontal and vertical directions with numerical time steps seen in Figure 9 was recorded, and the results are shown in Figures 10 and 11. With an increase in the thickness of the bottom coal, the position of the arch foot moved farther away from the roadway. When the thickness of the bottom coal was 0 m, 2 m, and 4 m, the position of the arch foot moved away from the roadway by 3 m, 3.5 m, and 4 m

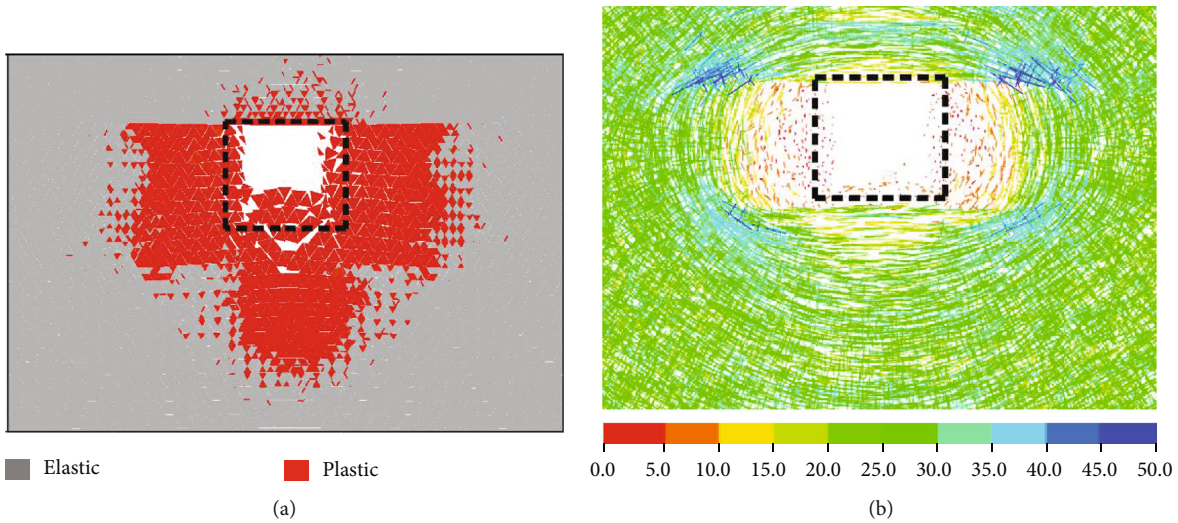

Figure 8: Reverse arching mechanism of the roadway floor. (a) Plastic zone and (b) stress tensors (MPa, colored by σ_1).

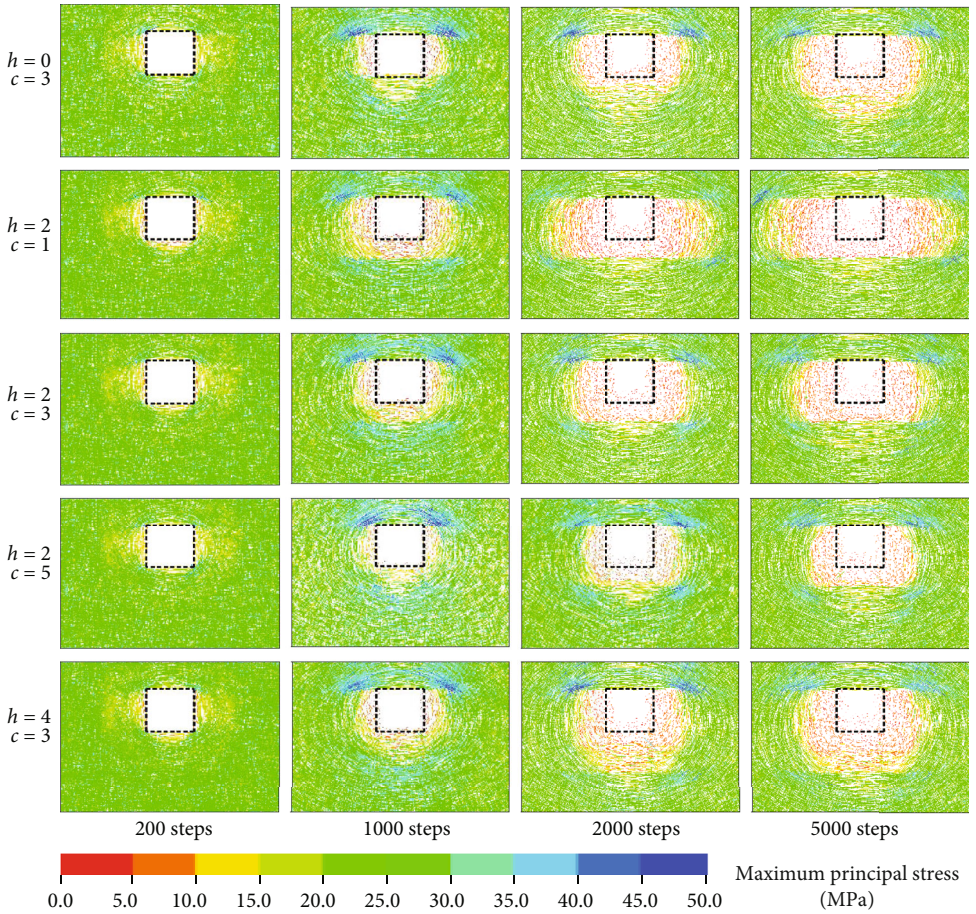

Figure 9: Time-varying evolution of stress tensor of the surrounding rock in the retained bottom coal roadway. Here, h = bottom coal thickness (m) and c = coal cohesion (MPa), the same as in Figures 10–13.

horizontally, and 1.7 m, 2.2 m, and 3.5 m vertically, respectively. With a decrease in coal strength, the position of the floor arch foot also moved away from the roadway. When the coal cohesion was 5 MPa, 3 MPa, and 1 MPa, the position of the arch foot moved away from the roadway 2 m, 2.3 m, and 2.3 m horizontally, and 2.8 m, 3 m, and 5.6 m vertically, respectively. The range and boundary shape of the surrounding rock failure was estimated based on the distance between the arch foot, the roadway side, and the arched structure of the floor.

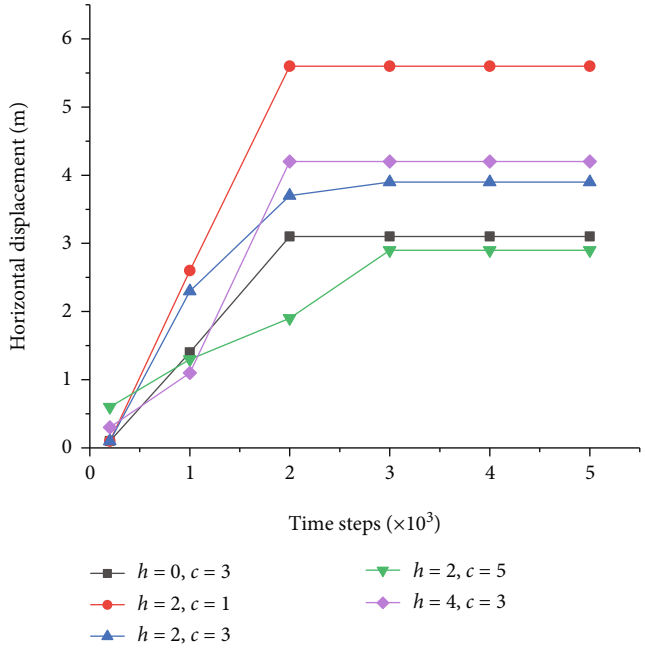

Figure 10: Horizontal displacement of the arch foot.

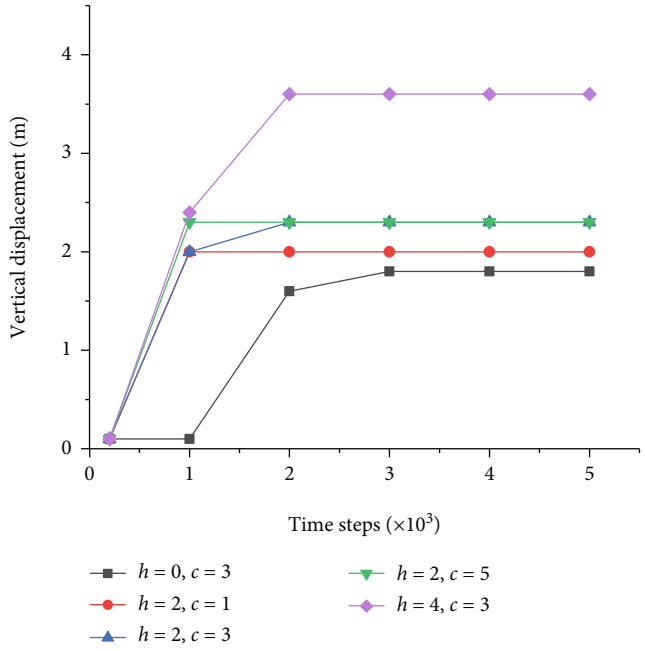

Figure 11: Vertical displacement of the arch foot.

Figures 12 and 13 show that the curve of the floor heave and displacement of the two sides of the roadway increased with time. The floor heave and displacement of the two sides of the roadway were consistent with the movement of the arch foot. The floor heave and displacement of the two sides of the roadway increased both with an increase in the thickness of the bottom coal and with a decrease in the strength of the coal body. The deformation of the two sides of the roadway and the floor stopped immediately when the arch foot stopped moving. The outward movement of the arch foot position implies that the failure range of the rock surrounding the floor arch increased, leading to an increase in the deformation of the roadway.

The stress concentration occurred on the surface of the roadway after excavation. Because of the unloading of the roadway surface, the surrounding rock in the shallow part was destroyed quickly, transferring concentrated stress to the deep part of the surrounding rock until it reached a balance with the strength of the surrounding rock. The induced effect of bottom coal on floor heave was that an increase in bottom coal thickness and a decrease in coal strength reduced the strength of the surrounding rock near the roadway surface, which was more likely to be destroyed under the action of concentrated stress. The concentrated stress was transferred deeper until a balance was reached with the deep surrounding rock of the roadway. Finally, both the depth of deformation and failure of the floor, as well as the width of the failure of the surrounding rock increased.

The shape of the failure boundary of the rock surrounding the floor was determined using the above simulation. The support of the roadway depended on the bearing capacity of the surrounding rock. The anchor cable should be anchored to the stable surrounding rock outside the floor arch. The support length of the anchor cable can be estimated using the arch foot positions shown in Figures 10 and 11. For example, when a bottom angle support is applied to the bottom coal of the roadway with a thickness of 2 m and cohesion of 3 MPa, the vertical and horizontal depths should not be less than 2.2 m and 3 m, respectively.

4.3. Migration Law of the Surrounding Rock of the Floor Arch of the Roadway with Retained Bottom Coal. In addition to the range and boundary shape of the floor rock failure, it was also necessary to investigate the deformation and migration of the surrounding rock in the arch to determine a reasonable support scheme.

Figure 14 shows the simulation results of the strata, plastic zone, and displacement of the five simulation schemes. Figures 15 and 16 present the layout of the four measuring points and their moving curves along the horizontal and vertical directions on the floor of the roadway with retained bottom coal.

As shown in Figure 15, following the excavation of the roadway, the measuring points on the floor moved significantly in the horizontal direction, with a maximum horizontal movement of 0.6 m. When the thickness of the bottom coal was 0 m, measuring points 2 and 3 were in the shallow part, which had horizontal displacement. In other cases, no horizontal displacement occurred at measuring points 2 and 3. However, the horizontal movement of measuring points 1 and 4 in the shallow part was significant. The horizontal movement of measuring point 4 was always the largest, approximately 0.3–0.6 m. Thus, the horizontal displacement of the floor rock generally occurred in the shallow part of the roadway rock. Therefore, the shear displacement of the shallow surrounding rock should be considered when setting the anchor cable support at the bottom corner, and the anchor cable support system should have a certain shear strength. Additionally, the horizontal displacement of

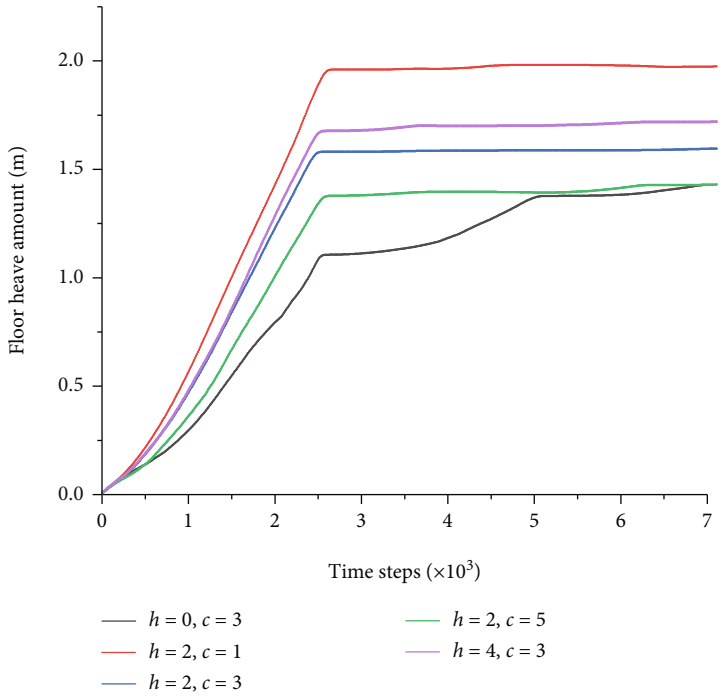

Figure 12: Floor heave amount.

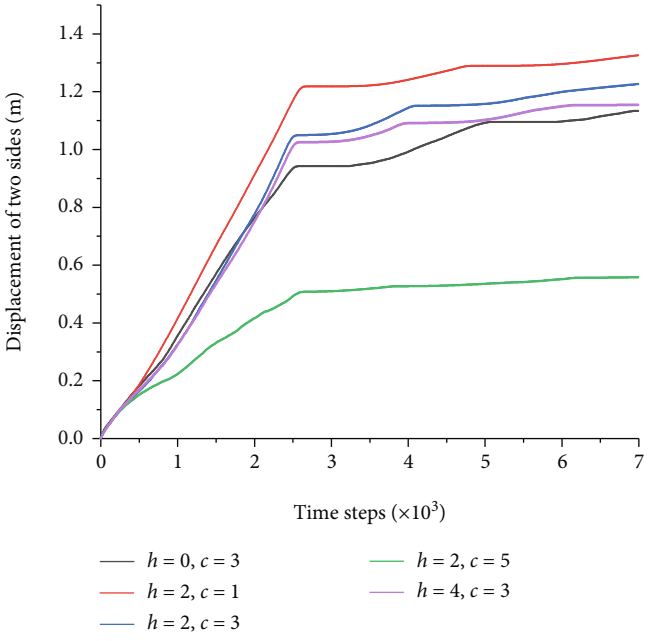

Figure 13: Displacement of two sides.

measuring point 1 first decreased, and then it increased, with time. The analysis shows that the surrounding rock at measuring point 1 moved to the two sides first, then to the middle line of the roadway. This finding is consistent with the conclusion from Section 4.2 that, under horizontal stress, the floor-surrounding rock first breaks in the middle of the roadway, moves to the two sides, then moves to the middle of the roadway. As shown in Figure 15(d), increasing the strength of the bottom coal can effectively control the horizontal displacement of the floor rock.

As shown in Figure 16, following the excavation of the roadway, the measuring points in the floor moved significantly in the vertical direction. The maximum vertical movement of measuring point 1 was approximately 0.9–1.4 m. The vertical movement of measuring points 3 and 4 under the two sides of the roadway was small, approximately 0.1–0.2 m. In Figure 16(a), measuring point 2 was in the shallow part of the surrounding rock and had a deformation of about 0.5 m. With an increase in the thickness of the bottom coal, the deformation of measuring point 2 decreased significantly to 0.2 m or less. Therefore, the shallow floor can be supported by an anchor or short anchor cable with a length of approximately 2 m.

In summary, the deformation of the floor-surrounding rock of the roadway with retained bottom coal mainly occurred in the shallow surrounding rock (approximately 2 m) close to the roadway surface. The floor-surrounding rock mainly migrated in the horizontal direction, whereas the roadway floor mainly moved in the vertical direction. The horizontal movement of the surrounding rock can be limited by setting an inclined anchor cable at the bottom angle, improving the shear capacity of the support with an anchor cable at the bottom angle, improving the strength of the surrounding rock at the bottom, or controlling the vertical movement of the floor with an anchor cable or short cable at the bottom angle.

4.4. Floor Heave Mechanism of the Roadway with Retained Bottom Coal. Because the supporting force provided by the supporting components is much smaller than the in situ stress in the surrounding rock, the existing supporting concept resists the in situ stress using the bearing arch structure of the surrounding rock in the roadway roof support. As

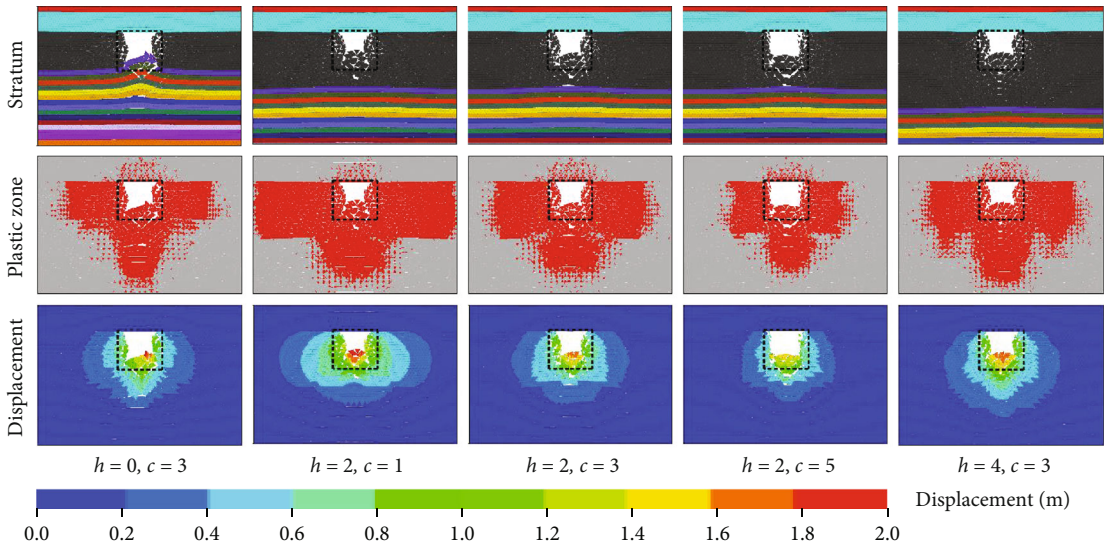

Figure 14: Simulation results of surrounding rock deformation of the roadway with retained bottom coal.

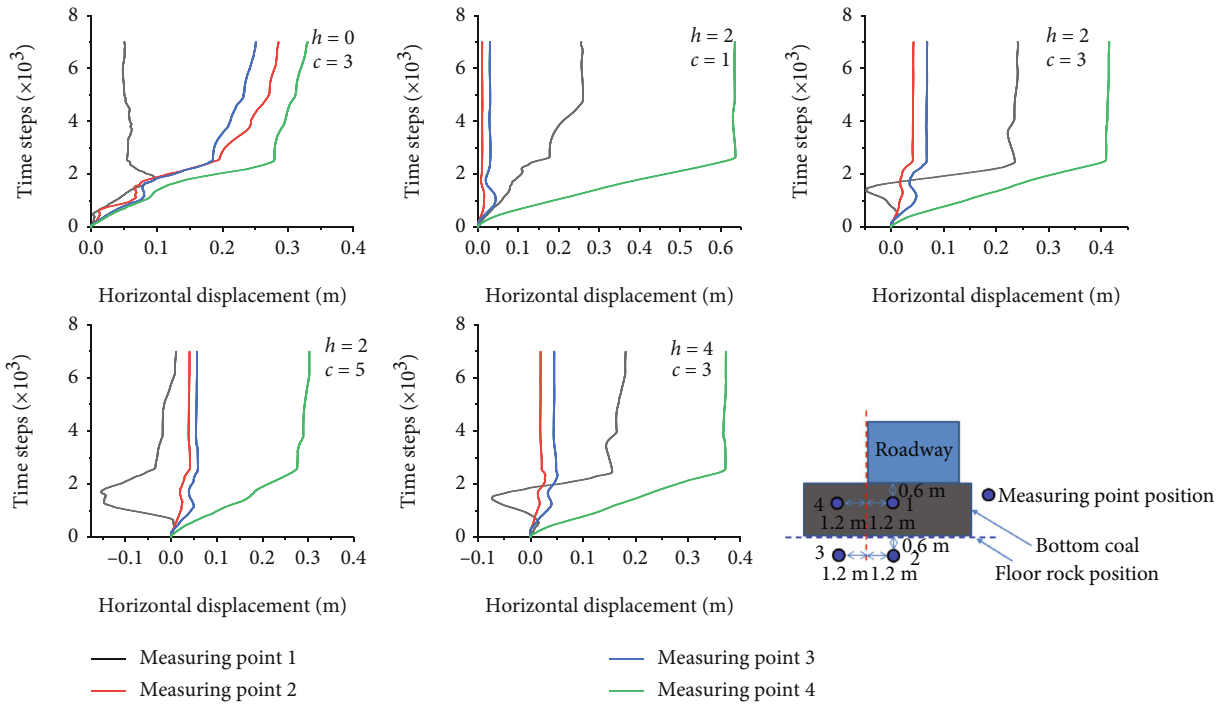

Figure 15: Curve of measuring point moving along the horizontal direction in the roadway floor.

mentioned above, the deformation and failure law of the floor under the action of in situ stress is similar to that of the roof, and, as shown in Figure 17, a floor arch structure is formed.

Under the condition of deep high stress, the plastic zone of the unsupported floor arch expands gradually until the stress and strength of the surrounding rock reach equilibrium. Compared to the arch of the supported roof, the floor arch, which is not constrained by the support system, expands outward significantly. The broken surrounding rock in the floor arch exhibits discontinuous deformation and moves toward the roadway. The larger the expansion range of the floor arch, the larger the expansion deformation of the surrounding rock in the arch, and, thus, the more significant the floor heave. Therefore, the unsupported floor is the main cause of floor heave in the deep coal roadway.

5. Engineering Practice

Based on this theoretical calculation and the numerical simulation, the supporting strategy of "high prestressed strong rock bolt (cable) supporting two sides and bottom corners in time" was proposed [42]. The supporting mode of the

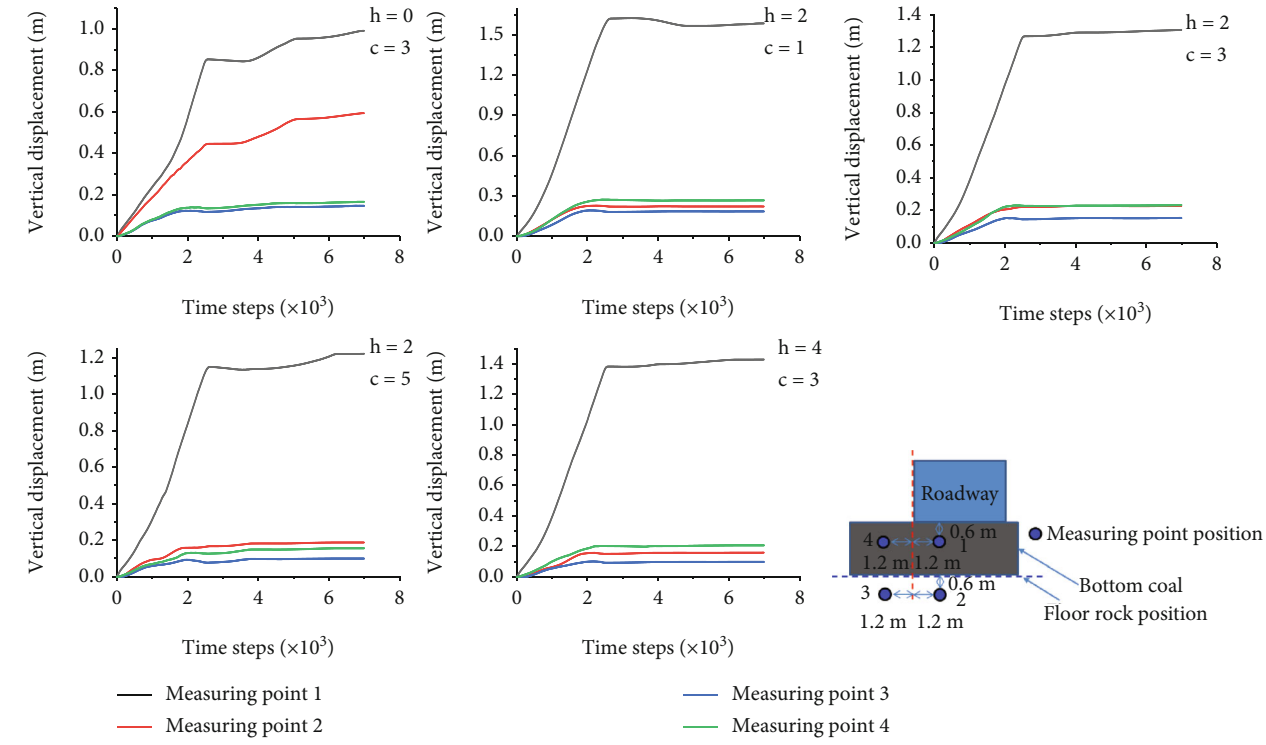

Figure 16: Curve of measuring point moving along the vertical direction in the roadway floor.

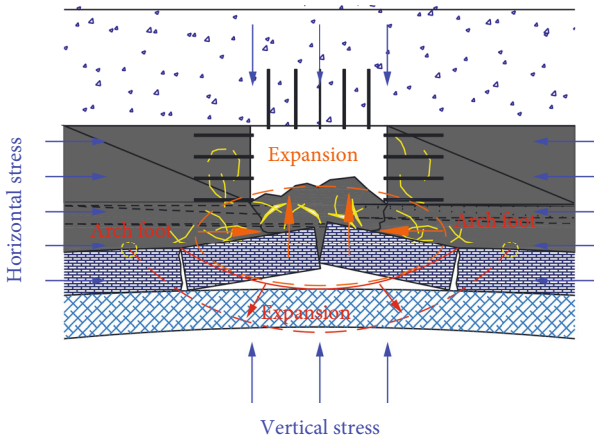

Figure 17: Evolution mechanism of the reverse arch expansion.

No. 020202 tailgate in the Qingyun mine was designed, and an industrial test was carried out in a new 100 m excavation section. The support strategy is illustrated in Figure 18. The support includes MG500 screw steel rock bolts with a length of 3000 mm, a diameter of 22 mm, and a preload of 70 kN, as well as cables with a 1 × 19 structure, a diameter of 21.8 mm, and a length of 6200 mm. The preload of the cables on the roof and the two sides was 300 kN and was 200 kN on the bottom corners. The cable support was used to limit the horizontal displacement at the bottom corners, and the rock bolt support was used to resist the horizontal shear displacement of the rock stratum; a W-type steel strip with a width of 280 mm was used for the roof, and a W-type steel guard plate with a width of 280 mm was used for the two sides.

As shown in Figure 19, the field test showed that both the displacement and the damage of the two sides of the No. 020202 tailgate were significantly reduced by strengthening the support of the two sides, increasing the bottom angle support, and adopting the timely prestressed anchor cable support. The maximum floor heave during the service period of the roadway was not more than 0.6 m (considering the cost, the economical and reasonable support scheme is designed on the premise that the roadway section meets the requirements of production and safety, although the deformation is still considerable), and there was no bottom lifting, confirming the feasibility of the support design.

6. Discussion

Floor heave is a complex engineering problem, especially for roadways with retained bottom coal. This paper analyzes this problem by establishing a Winkler elastic foundation beam model, and gives the floor heave mechanism and its influencing factors. It should be noted that the shallow part of the surrounding rock has entered the plastic stage, which is contrary to the assumption of the Winkler elastic foundation beam model. A lower foundation coefficient in the plastic zone than in the elastic zone is adopted to solve this problem, but errors exist. Then, the evolution mechanism of the roadway floor rock mass is analyzed by a discrete element numerical method, but the grid dependence is ignored. Finally, based on the laws obtained by the theoretical

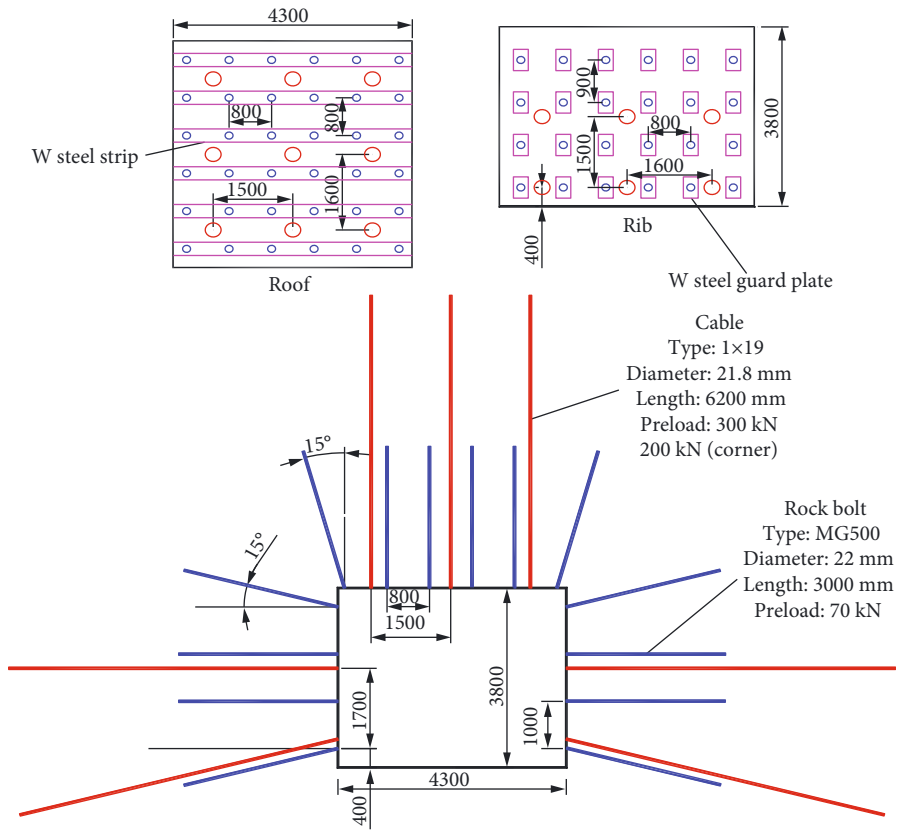

Figure 18: Support plan (mm).

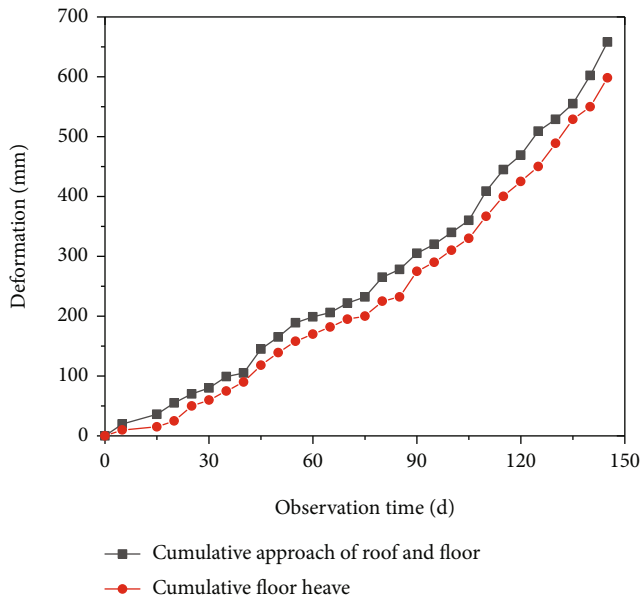

Figure 19: Deformation of No. 020202 tailgate in industrial test section during the service period (mm).

analysis and numerical simulation, a support scheme suitable for the No. 020202 tailgate in the Qingyun coal mine is put forward, which can provide reference for roadway support with similar geological conditions.

7. Conclusion

With an increase in the thickness of the bottom coal, the rigidity of the coal body (the foundation of the supporting rock layer) decreases, while the bending deformation range of the floor rock layer increases. This leads to an expansion in the range of the two sides of the coal body being squeezed by the floor rock layer, resulting in additional failure and deformation of the coal body sides. Therefore, the damage to the floor rock layer is extended and increased.

An increase in the bottom coal thickness and a decrease in the coal strength will decrease the surrounding rock strength near the roadway surface, which is more easily destroyed under a more concentrated stress. Thus, the concentrated stress should be transferred to the deeper part of the surrounding rock to achieve a balance with the unloaded surrounding rock in the deep part of the roadway. Finally, the depth of the floor deformation and failure increases, and the width of the failure surrounding the rock increases. The floor heave of the deep roadway is caused by expansion of the floor arch and surrounding rock. The increase in bottom coal thickness aggravates the expansion of the floor arch and causes greater floor heave deformation.

The support strategy of "high prestressed strong rock bolt (cable) supporting two sides and bottom corners in time" was proposed. After the excavation of the roadway, the prestressed strong rock bolt (cable) supporting the two sides of the roadway was applied in time, the inclined cable

was applied to the bottom corner of the roadway to limit the horizontal movement of the surrounding rock, and the bottom corner rock bolt was applied to improve the shear capacity of the bottom corner. Practice shows that this support scheme effectively controlled floor heave, and the feasibility of the support scheme was verified.

Data Availability

The data used to support the findings of this study are available from the corresponding authors upon request.

Conflicts of Interest

The authors declare no conflict of interest.

Acknowledgments

This research was funded by the National Key Research and Development Program of China (grant number 2017YFC0603003), the Applied Basic Research Project of Shanxi Province (grant number 201901D111049), and the Key Research and Development Projects of Shanxi Province (grant number 201903D321080).

References

[1] H. Kang, Y. Wu, F. Gao, J. Lin, and P. Jiang, "Fracture characteristics in rock bolts in underground coal mine roadways," *International Journal of Rock Mechanics and Mining Sciences*, vol. 62, pp. 105–112, 2013.

[2] M. Wang, N. Zhang, J. Li, L. Ma, and P. Fan, "Computational method of large deformation and its application in deep mining tunnel," *Tunnelling and Underground Space Technology*, vol. 50, pp. 47–53, 2015.

[3] Z. Wang, S. Yang, G. Xu, and Z. Wen, "Ground response and mining-induced stress in longwall panel of a kilometer-deep coal mine," *Shock and Vibration*, vol. 2021, Article ID 6634509, 14 pages, 2021.

[4] S. Yang, M. Chen, H. Jing, K. Chen, and B. Meng, "A case study on large deformation failure mechanism of deep soft rock roadway in Xin'An coal mine, China," *Engineering Geology*, vol. 217, pp. 89–101, 2017.

[5] D. Fan, X. Liu, Y. Tan, L. Yan, S. Song, and J. Ning, "An innovative approach for gob-side entry retaining in deep coal mines: a case study," *Energy Science and Engineering*, vol. 7, no. 6, pp. 2321–2335, 2019.

[6] Y. Jiang, Y. Zhao, W. Liu, and Q. Li, "Research on floor heave of roadway in deep mining," *Chinese Journal of Rock Mechanics and Engineering*, vol. 23, pp. 2396–2401, 2004.

[7] S. Mo, H. L. Ramandi, J. Oh et al., "A new coal mine floor rating system and its application to assess the potential of floor heave," *International Journal of Rock Mechanics and Mining Sciences*, vol. 128, 2020.

[8] K. Yi, Z. Liu, Z. Lu, J. Zhang, and S. Dong, "Effect of axial in-situ stress in deep tunnel analysis considering strain softening and dilatancy," *Energies*, vol. 13, no. 6, p. 1502, 2020.

[9] G. Zhao and S. Yang, "Analytical solutions for rock stress around square tunnels using complex variable theory," *International Journal of Rock Mechanics and Mining Sciences*, vol. 80, pp. 302–307, 2015.

[10] X. G. Zhao and M. Cai, "Influence of plastic shear strain and confinement-dependent rock dilation on rock failure and displacement near an excavation boundary," *International Journal of Rock Mechanics and Mining Sciences*, vol. 47, no. 5, pp. 723–738, 2010.

[11] K. Yi, Z. Liu, Z. Lu, J. Zhang, and Z. Sun, "Transfer and dissipation of strain energy in surrounding rock of deep roadway considering strain softening and dilatancy," *Energy Science and Engineering*, vol. 9, no. 1, pp. 27–39, 2021.

[12] X. Sun, F. Chen, M. He, W. Gong, H. Xu, and H. Lu, "Physical modeling of floor heave for the deep-buried roadway excavated in ten degree inclined strata using infrared thermal imaging technology," *Tunnelling and Underground Space Technology*, vol. 63, pp. 228–243, 2017.

[13] S. Mo, K. Tutuk, and S. Saydam, "Management of floor heave at Bulga Underground Operations—a case study," *International Journal of Mining Science and Technology*, vol. 29, no. 1, pp. 73–78, 2019.

[14] S. Liu, J. Bai, X. Wang, B. Wu, and W. Wu, "Mechanisms of floor heave in roadways adjacent to a goaf caused by the fracturing of a competent roof and controlling technology," *Shock and Vibration*, vol. 2020, 17 pages, 2020.

[15] Z. Ma, X. Liang, G. Fu, Y. Zou, A. Chen, and R. Guan, "Experimental and numerical investigation of energy dissipation of roadways with thick soft roofs in underground coal mines," *Energy Science and Engineering*, vol. 9, no. 3, pp. 434–446, 2021.

[16] S. B. Tang and C. A. Tang, "Numerical studies on tunnel floor heave in swelling ground under humid conditions," *International Journal of Rock Mechanics and Mining Sciences*, vol. 55, pp. 139–150, 2012.

[17] Y. Xu, E. Zhang, Y. Luo, L. Zhao, and K. Yi, "Mechanism of water inrush and controlling techniques for fault-traversing roadways with floor heave above highly confined aquifers," *Mine Water and the Environment*, vol. 39, no. 2, pp. 320–330, 2020.

[18] K. Yi, H. Kang, W. Ju, Y. Liu, and Z. Lu, "Synergistic effect of strain softening and dilatancy in deep tunnel analysis," *Tunnelling and Underground Space Technology*, vol. 97, p. 103280, 2020.

[19] J. Yang, G. Song, Y. Yang, and Z. Yang, "Application of the complex variable function method in solving the floor heave problem of a coal mine entry," *Arabian Journal of Geosciences*, vol. 11, no. 17, 2018.

[20] Q. Zhao, Y. Wang, Y. Liu, H. Li, J. Shi, and L. Shi, "The controlling techniques on floor heave of large cross section mining roadway with complicated surrounding rock," *Coal Engineering*, pp. 231–236, 2014.

[21] A. Ilinets, A. Sidorenko, and Y. G. Sirenko, "Computer modelling of a floor heave in coal mines," *In International Conference: Information Technologies in Business and Industry*, vol. 1333, p. 032028, 2019.

[22] L. Shi, H. Zhang, and P. Wang, "Research on key technologies of floor heave control in soft rock roadway," *Advances in Civil Engineering*, vol. 2020, 13 pages, 2020.

[23] C. Wang, G. Li, A. Gao, F. Shi, Z. Lu, and H. Lu, "Optimal preconditioning and support designs of floor heave in deep roadways," *Geomechanics and Engineering*, vol. 14, pp. 429–437, 2018.

[24] Y. Zhang, J. Shao, P. Chen, X. Li, and Z. Kan, "Development and application of mechanized control equipment for roadway

floor heave in coalmine," in *In Proceedings of the 2017 2nd Joint International Information Technology, Mechanical and Electronic Engineering Conference*, vol. 62, pp. 287–290, 2017.

[25] C. Liu, J. Ren, B. Gao, and Y. Song, "Support design and practice for floor heave of deeply buried roadway," *Iop Conference*, vol. 64, p. 12032, 2017.

[26] W. Zheng, Y. Zhao, and Q. Bu, "The coupled control of floor heave based on a composite structure consisting of bolts and concrete antiarches," *Mathematical Problems in Engineering*, vol. 2018, 14 pages, 2018.

[27] X. Zhang, T. Li, G. Chen, H. Liu, and P. Destech, "Study of floor heave mechanism in deep soft rock roadway," in *In 3rd Asian Pacific Conference on Energy, Environment and Sustainable Development*, pp. 164–167, 2017.

[28] X. Kang, D. Guo, and Z. Lu, "Mechanism of roadway floor heave controlled by floor corner pile in deep roadway under high horizontal stress," *Advances in Civil Engineering*, vol. 2021, 10 pages, 2021.

[29] G. Guo, H. Kang, D. Qian, F. Gao, and Y. Wang, "Mechanism for controlling floor heave of mining roadways using reinforcing roof and sidewalls in underground coal mine," *Sustainability*, vol. 10, no. 5, p. 1413, 2018.

[30] H. Xie, H. Zhou, D. Xue, H. Wang, R. Zhang, and F. Gao, "Research and consideration on deep coal mining and critical mining depth," *Journal of China Coal Society*, vol. 37, pp. 535–542, 2012.

[31] L. Wang and T. Ishihara, "A study of the effects of foundation uplift on the seismic loading of wind turbine tower and shallow foundation using a new dynamic Winkler model," *Engineering Structures*, vol. 219, 2020.

[32] G. Zhang, Y. Qu, X. Gao, and F. Jin, "A transversely isotropic magneto-electro-elastic Timoshenko beam model incorporating microstructure and foundation effects," *Mechanics of Materials*, vol. 149, p. 103412, 2020.

[33] L. Jiang, P. Zhang, P. Kong et al., "Rib-control support principle based on the foundation rigidity of coal mine roadways," *Journal of China Coal Society*, vol. 44, pp. 1020–1029, 2019.

[34] A. Bobet, "Elastic solution for deep tunnels. application to excavation damage zone and rockbolt support," *Rock Mechanics and Rock Engineering*, vol. 42, no. 2, pp. 147–174, 2009.

[35] A. Bobet and H. H. Einstein, "Tunnel reinforcement with rockbolts," *Tunnelling and Underground Space Technology*, vol. 26, no. 1, pp. 100–123, 2011.

[36] Z. Qin, *The Anchoring Mechanism of High-Strength Pressed Anchor and Time-Dependent Deformation Analysis of Bolted Rock Mass*, Institute of Rock and Soil Mechanics the Chinese Academy of Sciences, Wuhan, 2007.

[37] B. Huang, N. Zhang, H. Jing et al., "Deformation and failure characteristics and control technology of roadway surrounding rock in deep coal mines," *Journal of the China Coal Society*, vol. 2020, pp. 1–15, 2020.

[38] F. Gao and D. Stead, "Discrete element modelling of cutter roof failure in coal mine roadways," *International Journal of Coal Geology*, vol. 116-117, pp. 158–171, 2013.

[39] F. Gao, D. Stead, H. Kang, and Y. Wu, "Discrete element modelling of deformation and damage of a roadway driven along an unstable goaf—a case study," *International Journal of Coal Geology*, vol. 127, pp. 100–110, 2014.

[40] K. Yi, P. Gong, and C. Liu, "Overlying strata structures and roof control of working face under thin topsoil and thin bedrock in shallow seam," *Journal of China Coal Society*, vol. 43, pp. 1230–1237, 2018.

[41] S. S. Peng, *Coal Mine Ground Control*, John Wiley & Sons. Inc., New York, 2008.

[42] J. Chen, S. Yang, H. Zhao, J. Zhang, F. He, and S. Yin, "The analytical approach to evaluate the load-displacement relationship of rock bolts," *Advances in Civil Engineering*, vol. 2019, 15 pages, 2019.